Algal Research 90 (2025) 104183



Contents lists available at ScienceDirect

Algal Research

journal homepage: www.elsevier.com/locate/algal





Three non-invasive tools to estimate microalgal growth online and in real-time☆

Henrik Geltner[a,*], Sjoerd Kortstee[a], Maria Barbosa[a], Marcel Janssen[a]

[a] Bioprocess Engineering, Wageningen University and Research, P.O. Box 8129, 6700 EV Wageningen, the Netherlands

ARTICLE INFO

Keywords:
Bioprocess monitoring
Stoichiometric modeling
Microalgae
Photobioreactor
On-line monitoring
Photosynthethic quotient
Nitrate monitoring

ABSTRACT

On-line monitoring of bioprocesses is a cumbersome task that is relentlessly needed for accurate control and maximization of process efficiency, productivity, and yields. For microalgal processes, developing proper monitoring systems can be especially challenging due to their diverse characteristics. In this study, a novel approach is presented for non-invasively estimating microalgal growth in batch processes by online monitoring of the required nitric acid supply for pH control based on the proton stoichiometric imbalance of nitrate metabolism. Employing this strategy, we further increase measurement redundancy and estimate reliability by integrating gas analysis of carbon dioxide and oxygen fractions in the off-gas to determine biomass growth on-line. The obtained estimates of biomass concentrations were tested and validated in three autotrophic batch cultivations of *Tetradesmus obliquus* at a laboratory scale with a working volume of 1.8 L. All three online monitoring approaches could be employed for biomass estimation with outstanding results. Compared to offline measurements of biomass dry weight, correlation coefficients (R^2) of 0.96, 0.94, and 0.96 were achieved for the three monitoring methods. Differences in measurements of cell dry weight were determined to lie within 8 %, 7.1 %, and 6.7 % for normalized root mean square deviations (N-RMSD). The presented method of mass-balance-based growth determination proved suitable for real-time monitoring of microalgal biomass production. We believe this work paves the way for further process automation of the microalgal output by expanding on-line monitoring capabilities for biomass and cell state in parallel.

1. Introduction

Microalgae are a group of unicellular microorganisms that inhabit aquatic and terrestrial environments around the globe in abundance. As primary producers of organic matter, microalgae can grow through photoautotrophic utilization of sunlight as energy source and consuming CO_2 to build biomass. Aside from their essential role in the biological Carbon cycle within the global ecosystem, microalgae exhibit additional properties that make them interesting for use in various industrial sectors [1].

However, developing and optimizing microalgae processes for market implementation still poses numerous challenges. The efficient cultivation of microalgae requires adequate process controls that rely on monitored process variables for the continuous control of optimal process conditions [2]. Such high degree of process control is thereby important to guarantee product safety, applying good manufacturing and agricultural practices (GMP and GAP) [3].

For automation of such monitoring and control systems, measurement strategies that can be performed online or in situ are usually preferred over conventional analysis methods performed off-line or on-line [4]. Although the use of standard industrial sensors for most physicochemical process variables is widely established, only a few measurement options are currently available that allow for the online and real-time monitoring of biological parameters. In many cases, biological parameters are still determined by off-line analysis, which is laborious, time-consuming, and consequently unsuitable for automated process monitoring [5].

Many of the currently promoted techniques of bioprocess monitoring rely on measurements of optical properties by cell cultures or chemical components [6]. Optical sensing technologies are often easy to implement, as they typically provide straightforward options for calibration [6]. Also, their installation can be carried out either by directly submerging the sensor probes in a culture medium or sometimes by attaching them to the outer surface of transparent reaction vessels [4].

☆ This article is part of a Special issue entitled: 'DigitAlgaesation' published in Algal Research.

* Corresponding author.
E-mail address: henrik.geltner@wur.nl (H. Geltner).

https://doi.org/10.1016/j.algal.2025.104183
Received 31 March 2025; Received in revised form 30 June 2025; Accepted 1 July 2025
Available online 3 July 2025
2211-9264/© 2025 The Authors. Published by Elsevier B.V. This is an open access article under the CC BY license (http://creativecommons.org/licenses/by/4.0/).

However, several drawbacks and limitations of such sensors necessitate further development in the field of bioprocess monitoring. One of the limitations of optical sensing in upstream processes is its limited detection range, as a linear correlation between measurement signals and estimated process variables can often only be achieved at lower cell concentrations. Furthermore, biofouling on submerged sensor surfaces often disrupts accurate process monitoring over extended periods. Additionally, these sensors have struggled to differentiate between various cell states.

Recent advancements in the field have prompted a shift in research focus towards addressing some of the limitations inherent in current online monitoring practices. [7,8]. This shift has facilitated the development of innovative sensors [5] and advanced data processing methodologies, aimed at enabling precise segregated estimations of specific cellular compounds, including lipids and pigments [9,10]. Another focus of research lies in sensors that can be operated under versatile conditions, such as very high concentrations [11], as well as technologies to monitor non-invasively determining, for example, various characteristics of biofilm formation [8]. While some of those methods demonstrate promising results regarding achievable accuracy and measurement reliability their practicality and the actual value of information obtained may sometimes be questionable. For instance, one issue is the data density that may be required to calibrate multivariate models of such monitoring approaches. Another issue prevailing for use of optical sensors is the problem of sensor placement. This placement problem describes the dilemma of placing sensor probes at a representative, well-mixed location in the reactor while also shielding them from signal-disturbing influences such as gas bubbles or biofilm adhering to sensors. Especially optical sensing using immersed probes is sensitive to the light-refracting effects of gas bubbles.

To prevent systematic errors, alternative measurement principles should be developed that are suitable for replacing or complementing the current state of the art in bioprocess monitoring. In this context, elemental mass balancing-based methods demonstrate considerable potential. By measuring only the reaction rates of a set of key variables this strategy allow for to estimate unmeasured process variables through systems of mass balances and known stoichiometric relationships. Therefore, mass balancing-based monitoring provides the great advantage of not relying on mechanistic models or extensive knowledge of the underlying metabolism [12].

In microalgal cultivation, carbon dioxide and oxygen are two of the primary components involved in photosynthesis, alongside the biomass being produced. By measuring these production or consumption rates, one can determine the photosynthetic performance and subsequently estimate the growth of the microalgal cultures under autotrophic conditions, provided the stoichiometric relations of the growth process are known. So far, this has mainly been used in combination with specifically designed models and mathematical algorithms such as state estimators or observers [13]. The advantage here is the option of non-invasive installation at the gas exhaust side of reactors, thereby avoiding conditions that could disturb the measurement. Despite its sincere working principle and potential for real-time monitoring, this technology has not been developed to a state that enables its broad applicability as a viable alternative for real-time tracking of microalgae processes. One difficulty in setting up monitoring lies in a reliable estimation of the accumulation terms [12].

Considering the online monitoring of further growth-associated nutrient levels to determine biomass production, nitrogen-carrying nutrients play a significant role. Nitrogen is an essential nutrient for algae, and in the elemental composition of microalgae, it is one of the main constituents, alongside carbon and Oxygen, by mass. Furthermore, Nitrogen consumption and its depletion are closely related to significant changes in algal metabolism, triggering, for example, an enhancement of starch and lipid production in cells when nitrogen sources are depleted. Unfortunately, direct real-time monitoring of the most common nitrogen sources, nitrate and ammonium, is often not feasible. To date, attempts to monitor nitrate levels online have been focused mostly on leveraging optical sensing effects, including wavelength absorption, fluorescence spectrum analysis, and ion-selective membranes [5,14]. These sensors, therefore, face some of the same disadvantages as optical biomass sensors, such as sensor placement sensitivity to other light-associated effects, biofouling, or extensive chemometric model calibrations, among others. However, nitrate and ammonium exhibit more noticeable impacts that could be leveraged for measurement purposes, apart from the light-associated ones. The negative charge of nitrate, for example, affects the equilibrium of charge in aqueous solutions, which always manifests with net electroneutrality in the medium. The removal of negatively charged nitrates by algae affects the charge equilibrium in the solution, resulting in counter effects such as an equal consumption of positive charges. In other words, to take up nitrate, microalgae also need to take up an equal amount of opposite charge, primarily free protons (H+), to prevent the formation of a charge difference between cells and the medium. Consequently, in solutions, pH increases. In contrast, Ammonium consumption in microalgae cultures lowers the medium pH, as the uptake of positively charged Ammonium is accompanied by an equal removal of negatively charged hydroxide (OH-) ions, which is equivalent to a net release of protons (H+).

Exploiting this effect, Scherholz & Curtis proposed to control the process pH using a stoichiometrically-balanced growth medium design, which contains salt of Ammonium and nitrate in ratios that lead to the pH resettling around the setpoint after consumption of both nitrogen sources [15]. In this work, the authors further conclude that pH control and nitrogen supply can be successfully coupled by incremental addition of Ammonium and Nitrate ions, which could even improve the biomass yield on nitrogen [15]. This nitrogen uptake-related charge imbalance had further been studied by Wang & Curtis, who constituted a nearly equimolar proton imbalance for the consumption of nitrate or ammonium [16]. They also postulate that quantitative pH control by incremental nitrogen addition of nitrate or ammonium opens possibilities to assess nitrogen growth stoichiometry.

Conversely, given that the uptake of nitrogen occurs in a nearly constant ratio to total growth and Nitrate or Ammonium consumption is a significant factor contributing to pH dynamics, this means that the growth process of microalgae could be approximated by monitoring the number of respective nitrogen sources that are required to control pH at steady levels.

Continuous information on nitrate consumption rates are also interesting, since they could function as input in other monitoring approaches, for example, to predict microalgal lipid accumulation [17].

In this study, we thereby employ a strategy of feeding a nitric acid solution to control the process pH. Moreover, we continuously monitor process variables of pH, acid supply, and CO_2 levels in the gas fraction to estimate nitrate uptake rates and consecutively biomass formation. With this study we aim to reflect on the advantages and challenges of various approaches for online microalgal growth monitoring based on different elemental mass and charge balancing techniques, which enable the monitoring of several bioprocess variables in near real-time using non-invasive online measurements.

2. Material and methods

2.1. Precultivation

Cultures of *Tetradesmus obliquus*, formerly *Scenedesmus obliquus*, were pre-cultivated in shake flasks at 25 °C using an Infors HT Incubator. The pre-cultivation medium contained (in mM if not stated otherwise): 15 KNO_3, 1.5 K_2HPO_4, 10 $NaHCO_3$, 5 HEPES, 1 $MgSO_4*7H_2O$, 0.7 Na_2SO_4, 0.5 CaCl2*$2H_2O$, 0.08 Na_2EDTA, 0.028 NaFeEDTA, 0.019 $MnCl_2*4H_2O$, 0.004 ZnSO4*$7H_2O$, 0.0012 $CoCl_2*6H_2O$, 0.0013 $CuSO_4$, 0.0001 Na_2MoO_4 in adaption to [18]. The medium solution was adjusted to pH 7 by adding NaOH and steril-filtered using a 0.2 μm Sartorius Sartobran filter capsule. Illumination conditions in the incubator were

set to 150 μmol (photons PAR) m^{-2} s^{-1} incident light intensity, with a 16:8 h cycle of light: dark periods. Shaking was performed at 90 rpm, and ambient air was enriched with CO2 at 0.3%*v*/v. The shake flask cultures were grown for 18 days and were periodically diluted with 90 % v/v fresh medium every five days.

2.2. Cultivation experiment

2.2.1. Experimental set-up

The experiment was carried out in triplicate using three flat-panel photobioreactors (LabFors 5) from Infors HT, with a working volume of 1.8 L and a reactor depth of 2 cm each. The systems were equipped with a cooling jacket on one side of the reactor vessel and an LED wall for illumination on the other side. The reactor set-up is presented in Fig. 1 schematically. Aeration and mixing of cultures were achieved by sparging at a constant flow rate of 1000 mL min^{-1}. An installation for partial gas recirculation was instated to decrease the required rate of fresh gas streams by increasing the average retention time of the gas, as has previously proposed by Cuaresma et al. [19]. The total gas flow into the reactor consisted of a mixture of 196 NmL min^{-1} of fresh air (decarbonated), 4 NmL min^{-1} of CO2, and 800 NmL min^{-1} of recirculated gas from the reactor headspace. The inlet gas concentration was maintained at 2 % *v*/v CO_2 constantly throughout the process. The flow rates of the gas fractions were controlled using three dedicated mass flow controllers. For transport in the recirculation loop, a membrane pump was installed before the mass flow controller for recirculation. The gas mixture leaving the headspace was dehumidified using a condenser installed at the top of the reactor and cooled to 2 °C. After passing the condenser, the gas mixture was led through an additional glass vessel to capture condensate from the off-gas line. Subsequently, a T-piece partitions the dried gas into a recirculation flow and a system exhaust gas flow. The exhaust gas flow composition was analyzed using a connected Servomex Pro 4100 gas analyzer. The gas mixture was analyzed for its oxygen and CO_2 contents using a paramagnetic transducer for oxygen measurements and an IR sensor for CO_2 measurements. To prevent extensive pressure built up in the Reactor, a water lock was installed. This installation consisted of a 1 m long U-shaped tube filled with water to a height of 25 cm at ambient pressure. Overpressure in the reactors could thereby be estimated manually based on the height difference of water levels on the two sides of the tube.

Measurements of culture pH were performed in situ using an inpro3030 pH probe from Mettler Toledo. Control of pH was maintained at a level not exceeding seven by adding an acidic solution using a peristaltic pump. This solution for pH control comprised 0.5 mol L^{-1} nitric acid and 0.05 mol L^{-1} phosphoric acid. The addition of pH feed solution was determined throughout the experiment by placing the solution bottle on a laboratory scale from Sartorius and continuously monitoring its weight.

Data acquisition and logging of each reactor unit were conducted on separate computers. The logging of temperature, pH, and gas flow rates was done using the software tool Iris v5. Data from gas analyzers and balances were acquired and logged on a computer using a self-designed LabView application. The data from Hamilton sensors was logged on one computer running a Hamilton Arc Air application.

The cultivation medium contained (in mM if not stated otherwise): 5 KNO_3, 0.5 K_2HPO_4, 10 $NaHCO_3$, 1 $MgSO_4*7H_2O$, 0.7 Na_2SO_4, 0.5 $CaCl2*2H_2O$, 0.08 Na_2EDTA, 0.028 NaFeEDTA, 0.019 $MnCl_2*4H_2O$, 0.004 $ZnSO4*7H_2O$, 0.0012 $CoCl_2*6H_2O$, 0.0013 $CuSO_4$, 0.0001 Na_2MoO_4 in adaption to [18]. Before inoculation, the reactors were sparged, and a 0.5 M NaOH solution was added until the off-gas concentrations reached approximately 2 *v*/v% CO2, and the pH was set to 7. The required quantity of inoculum from pre-cultivation was determined by measuring the optical density (OD) at 750 nm of the shake flasks. An equal amount of medium was withdrawn from each reactor before inoculation. The amount of inoculate added was set to reach an optical density of approx. 0.5 at (OD_{750}). Cultivation conditions were set at 25 °C, with a sparging rate of 200 mL min^{-1} of fresh gas flow enriched with 2 % *v*/v CO2 and a pH setpoint of 7. A periodic illumination regime of 16:8 h of day and night was applied, respectively. The illumination intensity was controlled to provide 100 μmol (PAR) m^{-2} s^{-1} of incident irradiation (warm-white light) on the first day and 400 μmol (PAR) m^{-2} s^{-1} of incident irradiance from the second day onwards. Cultivation experiments were continued for 19 days.

2.2.2. Offline analysis

2.2.2.1. Culture sampling. Samples for offline analysis were periodically withdrawn from two of the three reactors. To determine OD_{750}, nitrate

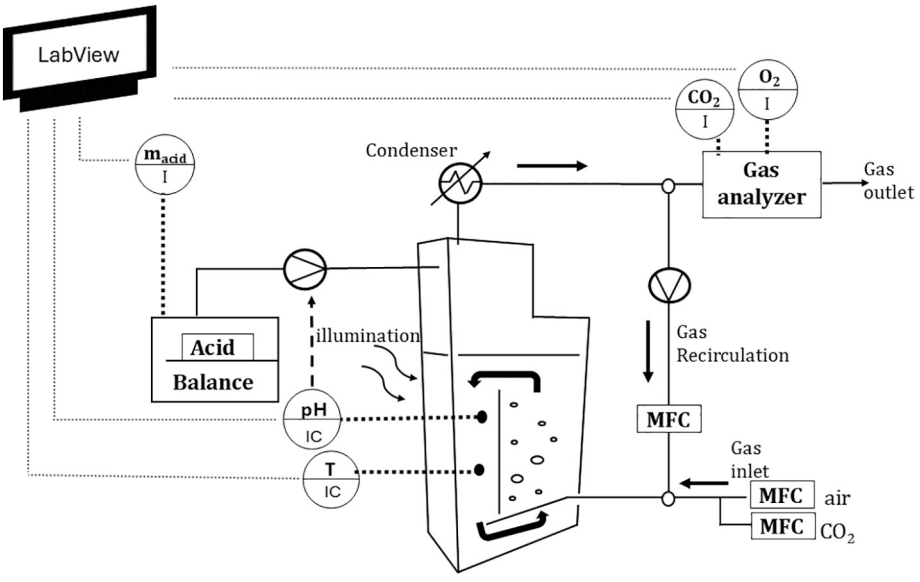


Fig. 1. Experimental set-up: flat panel photobioreactor equipped with sparging unit and sensors (pH & Temperature); one-sided illumination; gassing system of mixed gas inflow from controlled gas inlet streams (air & CO_2) and partial gas recirculation; Gas flows controlled via mass flow controllers (MFC); the gas-out line equipped with a gas analyzer for CO_2 and O_2 fractions; pH control (downwards) via acid addition; acid feed monitoring by a digital balance; Data Acquisition and logging via a computer and different DAQ & Logging applications.

and phosphate levels between 10 and 30 mL were taken from the reactors daily 15 min before the beginning of dark phases, excluding weekends. Sampling for dry weight analysis (DW) was carried out every 2–3 days. Measurements of OD_{750} and DW were determined directly following the sample withdrawal. The remaining sample volume was centrifuged for 10 min at 3100 rcf. The supernatant was withdrawn, filtered through a 0.2 μm pore size filter, and stored in the freezer at −20 °C in 15 mL Falcon tubes. Pellets from centrifugation were resuspended in demineralized water and centrifuged again at 3100 rcf for 10 min. The supernatant was discarded, and the pellets were stored in Eppendorf tubes at −20 °C in the freezer.

The third reactor, equipped with a Total Cell Density (TCD) sensor, was left without intermediate sampling. Here, the medium was only withdrawn twice to prevent overflowing due to acid additions.

2.2.2.2. Dry weight. Analysis of Dry weight concentration was conducted in triplicates every 2–3 days for two reactors. To determine the final Dry weight concentration of the last reactor, five samples were analyzed. Dry-weight samples were diluted with deionized water to 15 mL and then filtered using pre-weighed Whatman GF/F glass microfiber filters with a 0.7 μm pore size. Subsequently, the filters were rinsed three times with 15 mL of deionized water and dried in an oven at 105 °C for 24 h. The dried filters were placed in a desiccator for 30 min and weighed using an analytical balance. Dry weight concentrations were calculated as described in Eq. (1), where $c_{X,DW}$ is the weight concentration of dry biomass, m are the masses of the filter initially and after being loaded and dried and V represents the sample volume analyzed

$$c_{X,DW} = \frac{m_{filter,dried} - m_{filter,empty}}{V_{sample}} \quad (1)$$

2.2.2.3. Optical density. Optical density was determined in triplicate by measuring the absorbance of light at a 750 nm wavelength using a spectrophotometer (DR6000, Hach-Lange, USA). Before analysis, samples were diluted to achieve an absorbance of approximately 0.4–0.5 AU. The optical density at this wavelength (OD_{750}) was determined by multiplying the measured absorbance ($Absorbance_{750}$) of diluted samples times the respective dilution factor DF_{sample}, as shown in Eq. (2).

$$OD_{750} = Absorbance_{750nm} * DF_{sample} \quad (2)$$

2.2.3. Online analysis

2.2.3.1. Gas analysis and rate determination. The transfer rates of gaseous CO_2 (CTR) and O_2 (OTR) were estimated by measuring the volumetric fractions at the gas outlet and considering the total molar flow rates, assuming ideal gas behavior. Furthermore, by assuming instantaneous and perfect mixing, the transfer rates were then determined as the difference between molar flows entering and leaving the system, where F_{in} and F_{out} represent the total molar gas flow entering and leaving the system and $y_{i,j}$ represents the fraction of the respective gas compound i and stream j.

$$CTR = F_{in} * y_{CO2,in} - F_{out} * y_{CO2,out} \quad (3)$$

$$OTR = F_{in} * y_{O2,in} - F_{out} * y_{O2,out} \quad (4)$$

Before inoculation, the reactors were sparged at gas flows equal to those of the later experimental settings, and off-gas compositions were measured until a steady state was reached. The steady-state levels of carbon dioxide and oxygen, which are further referred to as wet-baseline values (WBL), were considered to reflect the expected composition of the gas mixture in the inlet ($y_{i,in}$) throughout the cultivations.

To account for possible variations of exhaust gas flows, we estimated total gas flows leaving the system using the data reconciliation approach proposed by Dabros et al. [9]. An adjustment was made to this calculation to exclude the water vapor fraction in the off-gas fractions (Eq. 5). This strategy was pursued since we determined the composition of the gas inlet in its wet state. As temperature and gassing rates were held constant throughout the process, we argue that continuous evaporation can be expected, with a corresponding constant offset due to the water content. As these errors are expected to be in both in- and outflow concentration readings, they should cancel out when determining the difference between these two flow rates (Eqs. (3) and (4)). Water vapor should thereby not affect our further determination of gas transfer rates. The total molar gas flow leaving the reactor (F_{out} (t)) was thereby calculated as shown in Eq. (5). There F_{in} represents the molar gas flow at the inlet, $y_{CO2,wbl}$ and $y_{O2,wbl}$ depict the molar gas fractions of CO_2 and O_2 in the wet baseline (saturated state), while $y_{CO2,exp}$ and $y_{O2,exp}$ are the molar gas fractions of CO_2 and O_2 at timepoint t during the experimental run.

$$F_{out}(t) = F_{in} \frac{1 - y_{O2,WBL} - y_{CO2,WBL}}{1 - y_{O2,exp}(t) - y_{CO2,exp}(t)} \quad (5)$$

For the final estimation of carbon uptake rate (CUR) and oxygen production rates (OPR), it was assumed that deviations in total dissolved inorganic carbon (DIC) and dissolved oxygen levels are negligible. Concerning the differences in time scales of gas transport rates and expected biological uptake rates, it can be approximated that transport rates equalize biological rates, as described in Eqs. (6) and (7).

$$CUR = CTR \quad (6)$$

$$OPR = -OTR \quad (7)$$

2.2.3.2. Nitrate uptake determination. The addition of Nitrogen was determined based on the weight reduction of the pH feed solution, measured continuously with an analytical balance. Logging of balance data was performed every 5 s. Approximating the dynamics of feed mass, we determined the weight loss over time due to acid addition in discrete steps using the gradient function in MATLAB. The measured weight was corrected for offsets at the time point and the moments when the bottle of acid solution needed to be refilled. The volumetric molar addition rate of the ($r_{NO3,add}$)was determined as presented in Eq. 8. Here dm/dt represents the weight gradients of the pH-feed solution over time $\rho_{pH,feed}$ is the density of the feed-solution $\rho_{pH,feed}$ and $c_{HNO3,pH\text{-}feed}$ is molar concentration of the solution. Furthermore, n_{NO3},add represents the molar quantity of NO_3 ions added and the effective reactor volume is given by V_R.

$$r_{NO3,add} = \frac{dn_{NO3,add}}{dt * V_R} = \frac{-\frac{dm_{pH,feed}}{dt} * c_{HNO3,pH-feed}}{V_R * \rho_{pH,feed}} \quad (8)$$

While the addition of nitric acid was controlled to regulate the process pH, this does not necessarily mean that nitrate addition rate and uptake rates are in balance. Generally, every deviation of charged ions can affect the pH parameter and thereby trigger an addition of nitrate. However, not every deviation in ions might be equally likely. That's why, for this process, a simplified model of charge balance dynamics was employed.

First, the electroneutrality constraint was built as described by the charge balance in Eq. (9).

$$[H^+] = [NO_3^-] + [HCO_3^-] + 2 * [CO_3^{2-}] + [OH^-] + \Delta[Ion_{Charge}] \quad (9)$$

where terms of $[H^+]$, $[NO_3^-]$, $[HCO_3^-]$,$[CO_3^{2-}]$ and $[OH^-]$ are the molar dissolved ion concentrations of hydrogen, nitrate, bicarbonate, carbonate and hydroxide and $\Delta[Ion_{charge}]$ summarizes the charge of all other dissociated ions, such as micronutrients. As described in Eq. (10), we assumed that dynamics in process pH were primarily due to fluctuations in total nitrate levels resulting from nitric acid addition and consumption, as well as deviations of bicarbonate and carbonate species. Lastly, hydroxide ions from the water equilibrium were also considered. The dynamic relation of this equilibrium constraint was

formulated as shown in Eq. (10) as the sum of time derivatives in molar concentration of each compound considered.

$$\frac{d[H^+]}{dt} = \frac{d[NO_3^-]}{dt} + \frac{d[HCO_3^-]}{dt} + 2^*\frac{d[CO_3^{2-}]}{dt} + \frac{d[OH^-]}{dt} \quad (10)$$

Subsequently, the free proton concentration ([H^+]) and it's derivative were estimated from pH measurements throughout the process, assuming an activity (γ_{H+}) of one (Eq. (11)).

$$[H^+] = 10^{-pH} \quad (11)$$

The hydroxide concentrations were calculated assuming equilibrium with water (eq. 12).

$$K_W = [OH]^- [H^+] = 10^{-14} \quad (12)$$

Regarding the carbonate-buffer system, although it more accurately consists of three steps, the buffer system is often described in two steps only. This model omits a step in which carbonic acid (H_2CO_3) is formed from water and dissolved carbon dioxide. However, since the equilibrium between carbonic acid and dissociated bicarbonates is usually far on the bicarbonate side, it is often summarized together with the dissolved $CO_{2,liq}$ fraction in an adjusted term of $CO_{2,liq}$* for reasons of simplicity. The carbonate-buffer model and it's dissociation equilibrium were therefore formulated as shown in Eqs. (13) and (14). Equilibrium constants of bicarbonate K_1 and carbonate K_2 were obtained for standard conditions from [20]. This was assumed to be representative without adjustment because the experimental conditions employed in this study did not differ considerably from these standard conditions. For simplification it was assumed that the salinity of the utilized freshwater medium and a slight overpressure in the reactor of approx. 18–20 mbar were negligible.

$$CO_{2,liq}{}^* \rightleftharpoons H^+ + HCO_3{}^- K_1 = \frac{[HCO3^-]\,[H^+]}{CO2,liq} = 10^{-6.35} \quad (13)$$

$$HCO_3{}^- \rightleftharpoons H^+ + CO_3{}^{2-} K_2 = \frac{[CO3^{2-}][H^+]}{[HCO3^-]} = 10^{-10.33} \quad (14)$$

A common practice in modeling and simulation of the carbonate system is to assume equilibrium with the dissolved CO_2 in the liquid. This term is, however, often subjected to fluctuations driven by limitations of gas transports to the liquid or sudden changes in the biological behavior of CO_2 uptake. For this reason, also bicarbonate or carbonate levels might, in fact, undergo changes. Modeling dynamics of those bicarbonate and carbonate levels can be accounted for through partial differentiation of equilibrium assumption.

$$\frac{d[HCO_3^-]}{dt} = \frac{K_1{}^*\partial[CO_{2,liq}]}{[H^+]\,\partial t} - \frac{K_1\,[CO_{2,liq}]^*}{[H^+]^2}\,\frac{\partial[H^+]}{\partial t} \quad (15)$$

$$\frac{d[CO_3^{2-}]}{dt} = \frac{K_1K_2{}^*\partial[CO_{2,liq}]}{[H^+]^2\,\partial t} - 2\,\frac{K_1K_2\,[CO_{2,liq}]^*}{[H^+]^3}\,\frac{\partial[H^+]}{\partial t} \quad (16)$$

Levels of dissolved CO_2 in the medium ($CO_{2,liq}$) were estimated from the carbon transfer rate using Eq. (17). The mass transfer coefficient (k_La) of the system was determined prior through the static gassing-out method [21].

$$\frac{CTR}{k_{La}} + C^*_{CO2,liq} = C_{CO2,liq} \quad (17)$$

Next, nitrate dynamics are assessed. Being a strong acid, nitric acid is assumed to dissociate into its ions when added to the medium completely. Its evolution is, therefore, solely dependent on the rates of volumetric uptake ($rNO_{3,uptake}$)and addition($r_{NO3,add}$), as depicted in Eq. (18)

$$\frac{d[NO_3^-]}{dt} = r_{NO3,add} - r_{NO3,uptake} \quad (18)$$

By inserting constants and equations from Eqs. (13)–(18) into Eq. (10) and restructuring differential terms, the nitrate uptake rates can be calculated from data on nitrate addition rates, dissolved CO2 levels, and process pH over time.

$$r_{NO3,uptake} = r_{NO3,addition} + \frac{\partial[CO_{2,liq}]}{\partial t}\left(\frac{K_1}{[H^+]} + \frac{K_1K_2}{[H^+]^2}\right) + \frac{\partial[H^+]}{\partial t}\left(-1 - \frac{K_1\,[CO_{2,liq}]}{[H^+]^2} - 2^*\frac{K_1K_2\,[CO_{2,liq}]}{[H^+]^3} - \frac{K_W}{[H^+]^2}\right) \quad (19)$$

2.2.3.3. Biomass estimation. To link rates of elemental uptake or production to the formation of total biomass, a stoichiometric model composition was required that defines the respective content of each element in biomass. The amount of individual elements in the biomass can vary between different strains and their metabolic state. Therefore, it is difficult to derive generic composition models, as it is unclear under which environmental conditions an ideal cell state with representative character can be assumed. Additionally, the determination of such models involves a multitude of different analytical measures, each with its proprietary degree of possible accuracy that can be achieved. In this study, we used the stoichiometric model composition shown in Eq. (3) normalized to 1C-mol, which had been proposed by Kliphuis et al. for the photoautotrophic growth of *Chlorella sorokiniana* on nitrate as a nitrogen source [22]. In this case, a constant elemental composition of biomass is assumed throughout the process.

$$CO_2 + 0.93{\cdot}H_2O + 0.15{\cdot}NO_3^- \rightarrow CH_{1.7\pm0.01}O_{0.40\pm0.02}N_{0.15\pm0.004} + 1.42{\cdot}O_2 + 0.15{\cdot}OH^- \quad (20)$$

The estimation of biomass concentrations was carried out based on the stoichiometric model Eq. (22), utilizing the determined rates of carbon dioxide uptake, oxygen production, and nitrate uptake. The production rate for C-molar biomass was obtained considering the ratio of stoichiometric coefficients between measured process rates and algal production derived respectively, shown in Eq. (21). Here, $r_{Cmol,X}$ represents the C-molar, volumetric rate of biomass growth, r_i is the volumetric conversion of a reactant i and v are the respective stoichiometric coefficients of biomass (Cmol,X) and reactant i from the growth model Eq. (20).

$$r_{Cmol,X} = r_i \cdot \frac{\nu_{Cmol,X}}{\nu_i} \quad (21)$$

The biomass concentration was subsequently calculated by integrating the logged rates and adjusted for the starting concentration, as shown in Eq. (22), where c_X is the biomass concentration at timepoints t and t_0, MW is the molar weight of 1C-mol biomass and r is the volumetric rate of biomass growth. The molar weight per carbon-mol of biomass used in this study was 23.682 g_X C-mol^{-1} as had been previously determined by Kliphuis et al. [23].

$$c_X(t) = c_X(t_0) + MW_{Cmol,X} \cdot \int_{t_0}^{t} r_{Cmol,X}(t)\,dt \quad (22)$$

2.3. Statistical analysis

To determine the accuracy and reliability of the online estimations, a comparison was made with measurements of dry weight concentration. The coefficient of determination R^2 value is used to indicate the degree of agreement between results obtained by the two distinctive methods. This coefficient was derived for the dataset of two cultivations combined

to describe the robustness of this method. In addition, the R^2-values of individual cultivation datasets were determined to elaborate individual performances and the potential of this method. Lastly, datasets of biomass predictions by the online monitoring approaches were fitted against measured Dry Weights, and R^2 values were determined again for the fits in order to identify possible bias.

$$R^2 = 1 - \frac{\sum (y_i - \hat{y}_i)}{\sum (y_i - \bar{y}_i)} \tag{23}$$

Furthermore, a normalized root mean square deviation factor (NRMSD) is used to assess the relative accuracy between biomass estimates from online measured rates of carbon uptake, oxygen production, and nitrate uptake, and results from off-line dry weight analysis.

$$NRMSD = \frac{\sqrt{\frac{\sum (y_i - y_i)^2}{n}}}{y_{max} - y_{min}} \tag{24}$$

3. Results & discussion

3.1. Process dynamics

Analysis of the process variables, including pH, off-gas CO2 concentration, and balance data, as depicted in Fig. 2, reveals that all three cultivation setups exhibited high synchrony during the initial seven days. However, a failure in the control regime of the third reactor led to a temporary suspension of daily illumination on the 7th day, resulting in the culture being maintained in darkness for approximately 32 h. Notwithstanding this disruption, the cultivations in the other two reactors continued to progress synchronously, maintaining coherence through the duration of the experiment, which spanned 18 days.

During the experiments, it was observed that pH and CO_2 levels oscillated periodically between day and night phases. The pH reached minimal values of around 6.78 during the 8-h night phases and values of pH ~7.01 during the day phases. The solely acid-based pH-control strategy was thereby successfully omitting pH levels from rising significantly over the setpoint of 7. Nevertheless, the decreases in pH that occurred at night could not be countered by further acid addition, which led to unregulated pH dynamics below the setpoint during the night. This can be seen in the extended dark phase of the third reactor on day 7 it pH and CO2 levels remained relatively constant (Fig. 2) compared to the other two reactors were the illumination regime remained uninterrupted. As previously mentioned, CO2 concentrations in the off-gas also oscillated between the day and night phases. The simultaneous swinging of the pH parameter is a consequence of the oscillating CO_2 levels in the gas phase. Carbon dioxide dissolves in aqueous solutions until an equilibrium is reached between the concentrations in the gas and liquid phases. This equilibrium between the gas and dissolved fractions of volatiles depends on various parameters but can be assumed to be linearly dependent in systems of constant temperature, total pressure, and salinity. As formulated by Henry's law (Eq. (25)) the saturation concentration (C*) of a volatile compound i in the liquid can be described as linearly depending on the respective partial pressure p_i in the gas and a compound specific pseudo-constant (Henry-constant of i under specific conditions of Temperature T and Salinity S)

$$C^*_{i,liq} = p_i{}^* H_i^{c,p}(T,S) \tag{25}$$

where $C_{i,liq}$ is the concentration of molecule species (i) in the liquid phase, p_i is the partial pressure of compound i in the gas phase and $H_i^{c,p}(T,S)$ is the specific Henry constant dependent on the temperature and salinity of the solution. The levels of dissociated bicarbonate and carbonate are dependent on the concentration of dissolved carbon dioxide. Carbon dioxide reacts with water, forming carbonic acid that

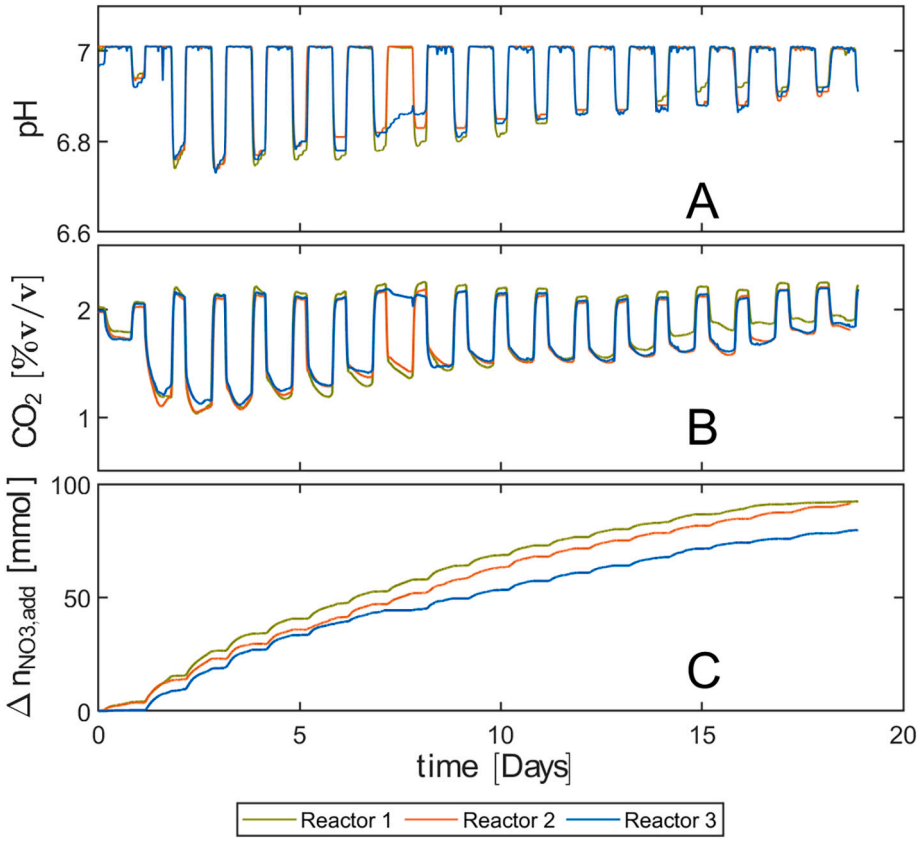


Fig. 2. Online monitored process dynamics of (A): pH; (B): off-gas CO2 concentrations and (C): total molar addition of nitrate observed in three photoautotrophic cultivations of T. obliquus with illumination cycles of 16:8 hours (Day: Night); employing nitric acid for pH-control.

further dissociates to form bicarbonate (HCO_3^-) or carbonate (CO_3^{2-}), releasing one or two protons in the process, respectively (Eqs. (14), (15)). Consequently, the solution is acidified. Inversely, if dissolved carbon dioxide levels decrease, pH rises. This network of equilibrium reactions is known as the carbonate system. The system depends on a multitude of process variables such as temperature, ambient pressure and partial pressure of gaseous CO_2 as well as ionicity of the medium.

Initial concentrations of carbonate species $CO_{2,liq}$, HCO_3^-, and CO_3^{2-} were estimated assuming an equilibrated state by using Eq. (25) for the dissolved CO_2 and Eqs. (13) and (14) for bicarbonate and carbonate levels, respectively. Next, transiently changing process concentrations of the three compounds were determined considering the equilibrated state at timepoint t_0 and the dynamic relations described in Eqs. (15)–(17). The obtained results are displayed in Fig. 3.

Fluctuations of observed for gaseous carbon dioxides can be explained by to the circadian rhythm of microalgal metabolism and alternating phases of day and night. During day phases, microalgal photosynthesis dominates. Light energy is harvested in the chloroplast to bind CO_2 [24]. Subsequently, the consumption of dissolved CO_2 in the medium creates a disbalance between dissolved and gaseous CO_2 concentrations, leading to a net flux of CO_2 from the gas to the liquid phase in order to reestablish equilibrium. Consequently, CO2 levels in the gas and medium are lowered when photosynthesis is active also causing a decrease in the levels of bicarbonate. In darkness, photosynthesis can't prevail, and levels of dissolved CO_2 rise again due to the continuous sparging. In addition, microalgae consume sugars to generate necessary energy in the form of ATP for processes of maintenance and growth-related respiration [23]. In this process of dark respiration, oxygen is consumed to decompose the sugars and release energy which produces carbon dioxide in the way.

The dissolved CO_2 is enriched in the medium. A sharp rise of dissolved inorganic carbon and associated compounds during the transition from day to night phases thereby occurred, which can be observed by the estimated levels of carbonated molecules species shown in Fig. 3. As DIC increases more CO_2 is released from the liquid into the environment which can also be observed in Fig. 2, where carbon dioxide levels in the off-gas phase exceed the 2 % *v*/v of the inlet gas stream during periods of 8 h darkness. After each system perturbation at day/night transition saturating phases can be observed where only minuscule changes of measured CO_2 in the off-gas or estimated DIC levels occur. In these states, which make up a majority of total process time, the driving force for transport between dissolved CO_2 and its gaseous counterpart is high enough so that the transport rates between gas and liquid phases equals the formation or consumption rates of carbon dioxide and oxygen [23].

An additional aspect that likely had contributed to increased interactions between pH and carbon dioxide consumption was the installation of a gas recirculation loop. By implementing partial gas recirculation the average retention time of gas molecules in the system was increased. This allowed for CO_2 to be used more efficiently in the process, as gas flows at the inlet and outlets could be held low. Hence, less CO_2 was wasted.

Increasing the retention time of gases also amplifies differences between incoming and outgoing gas fraction levels as the saturation speed driven by fresh gas flows is reduced. On the one hand, this amplifying behavior can be seen as a beneficial asset because the gas level deviation resulting from a biological activity is increased, in contrast to the expected signal noises of gas analysis. On the other hand, pH equilibria are affected more strongly. Regarding the additional objective of estimating nitrate uptake rates on the basis of the charge balance, this must be considered with particular care.

During dark phases of cultivation no acid, and thus nitrate was added, as can be followed from the nitric acid addition data depicted in Fig. 2 Cd. The pH value at this time had decreased below the setpoint due to the enhanced CO_2 and bicarbonate concentrations. This prevented any further need for the addition of nitric acid, even though nitrate consumption might have taken place. The information on nitric acid addition from balance data is thereby not sufficient to assess behaviors of nitrate accumulation by microalgae continuously over day and night periods. However, the influencing of dynamics of carbonic ion deviations could be accounted for to enable continuity of nitrate estimations also at dark phases using data on pH and off-gas CO_2.

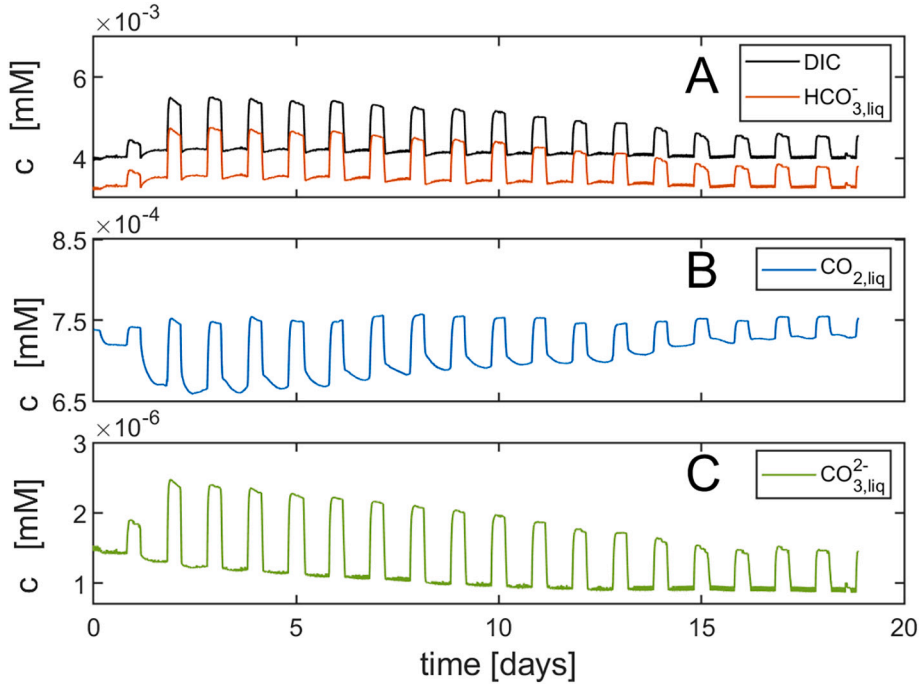


Fig. 3. Estimated concentrations over time of dissolved carbonate species during a diurnal cultivation of T. obliquus (16:8 h, Day:Night) [A]: estimated levels of total Dissolved Inorganic Carbon (DIC) and bicarbonate (HCO3-); [B]: estimated levels of dissolved CO2; (C): estimated levels of carbonate ion levels; estimations derived from the off-gas measured CO2 and inlet CO2 concentrations and pH of culture broth.

3.2. Monitoring biologic conversion rates

The monitoring of biologic conversion rates is an important key aspect for bioprocesses industries. Knowledge of the maximally achievable conversion rates is indispensable in order to predict total productivity and process costs and determine the economic feasibility of production processes.

Identifying the required process conditions helps to develop novel process control strategies boosting production, reducing costs, or maintaining a specific product quality. Furthermore, investigating characteristics of process rates in response to environmental triggers can also be used to gain better understanding for certain metabolic functions and their regulation within cells. This can, for example, be utilized to identify metabolic bottlenecks with the objective to later manipulate them, for example, via genetic engineering.

The on-line monitored rates of carbon uptake and oxygen production of the three autotrophic batch cultivations are shown in Fig. 4. Over the process, rates in all three reactors showed similar trends, indicating that comparable growth has been achieved. Maximal rates at days reached mostly similar heights, with the exception of reactor 3 on the seventh day, when no illumination of the culture was carried out.

On the first day, both CUR and OPR in day and night phases were considerably lower than during the rest of the process. This can be attributed to the lower light intensity that was used on the first day. The light intensity during this first illumination period was set to ~100 µmol PAR m^{-2} s^{-1} instead of the later 400 µmol PAR m^{-2} s^{-1}, allowing cultures to adapt incrementally to dilute conditions in the reactor. This was necessary to avoid initial photo inhibition.

In dense cultures, mixing ensures that cells experience fluctuation of over and under-saturating light conditions. Under these conditions, most microalgae adapt their photosynthetic apparatus to maximize the possible harvest of light energy based on the average light intensity available. However, a sudden dilution, for example, during inoculation, changes the average reactor conditions to light being excessively available for each cell. The excessive photon energy cannot be harvested fast enough, which leads to photosystems being inactivated or even damaged [25].

After inactivation, many photosystems can be repaired by microalgae through a pathway called the PSII repair cycle ([24,26] [25]). This process, however, requires additional energy. Overall, such photo inhibition processes affect productions negatively, for example, by extending the lag phase where basically no growth occurs.

After the first day of cultivation, the settings of light control were switched to supply a light intensity of 400 µmol PAR m^{-2} s^{-1} in block over 16 h per day. In response, carbon uptake and oxygen production rates increased from the second day on.

After the third day, the maximal daily conversion rates began to decline again. At this time, the biomass densities had reached a state in which an increasing amount of the culture volume was not illuminated sufficiently anymore. Shading by the cells located in the front layers of the reactor prevented light photons from reaching deeper into the reactor volume. In these shaded zones, microalgae may start to carry out dark respiration even during the day. The respiration process releases CO_2 and requires consumption of O_2. Hence, net volumetric conversion rates of carbon dioxide and oxygen are seen to diminish with further expansion of the shading zone. After approximately three to four days, declines in net conversion rates appear to decelerate. A prolonged and nearly constant net uptake of CO_2 and associated oxygen production was established until the 15th day of the cultivation. Most likely, light acclimation of cells during this period affected light attenuation and efficiency of light use as cells adapt to, on average, lower light availability.

Ultimately, light intensity no longer suffices to promote the growth of cultures. This is depicted by another reduction in net process rates from day 15 onwards. On the 19th day, the experiments were stopped, although net bioactivity had not yet fully ceased. Similar to the daily photosynthesis rates that were monitored, respiration at night also seemed to deviate between the different phases of light-limited batch growth.

Another metric to determine the relative efficiency of photosynthetic growth versus respiration is the photosynthetic quotient (PQ). This ratio compares the rates of oxygen release and carbon dioxide consumption. The parameter can be leveraged as an indicator for additional product formation or consumption of carbon sources aside from CO_2 [23]. Eriksen et al. demonstrated that PQ can be used to determine the degree of oxidation in biomass, which indicates compositional changes such as increased starch accumulation by microalgae [27]. The obtained results of PQ values are displayed in Fig. 5.

As depicted in Fig. 5, the PQ ratios fluctuated periodically, with higher values observed during the day and lower values at night. This was expected due to photosynthesis being predominant over respiration in growth phases. At the start of each day phase, sharp spikes in PQ can be observed. Following up, the PQ decays and approaches a plateau.

At days, PQ settles at plateaus around 1.4 mol_{O2} mol_{CO2}^{-1} after the

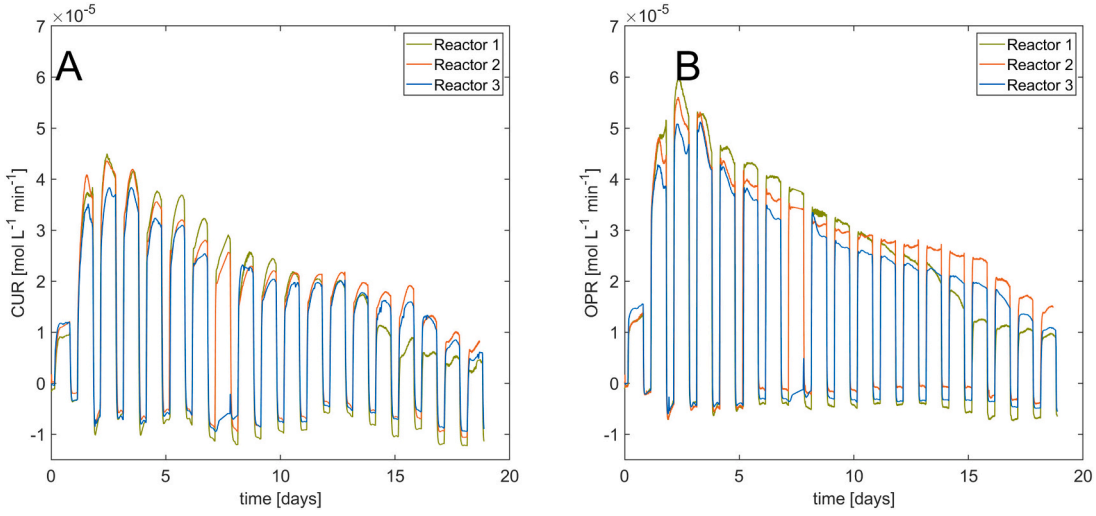


Fig. 4. On-line estimated gas conversion rates in three autotrophic batch cultivation of T. obliquus (illumination at 16:8 hours light: dark; blockwise); (A): carbon dioxide uptake rates (CUR) and (B): Oxygen production rates; estimations based on continuous off-gas analysis and known concentrations of oxygen and CO_2 in the inlet gas stream.

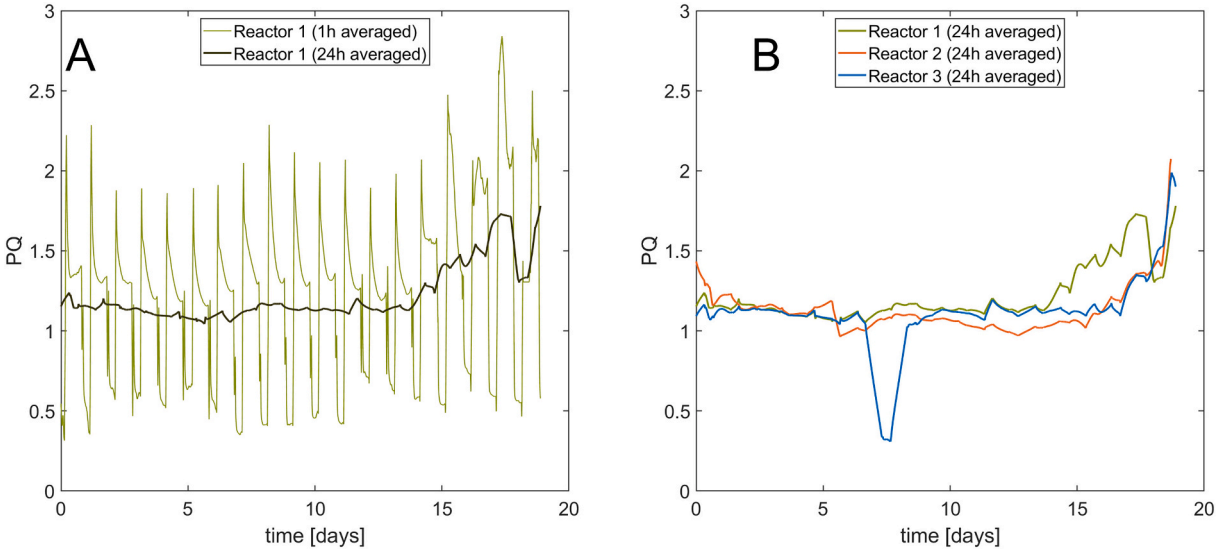


Fig. 5. Photosynthetic Quotients determined by off-gas analysis during batch-wise autotrophic cultivations of Tetradesmus obliquus in flatpanel photobioreactors under 400 μmol_{PH} (PAR) m^{-2} s^{-1} incident light and 16:8h (Day: Night) light regime; (A): hourly and 24 hourly averaged PQ in Reactor 1; (B): 24 hourly averaged PQ in three parallel cultivations.

initial daily spikes that reach up to 2–2.5 mol_{O2} mol_{CO2}^{-1} approximately. At night, a sudden decrease in PQ is seen that ultimately levels in a range of approximately 0.47–0.7. These observations align with other findings on PQ values reported in the literature [22,23,27]. For continuously illuminated cultures of *Chlorella sorokiniana* Kliphuis et al. reported that PQ values stabilized at ~1.4 and shortly shifted when illumination was increased [23]. In another study, maximal PQs of ~2.2 had been reached after the beginning of illumination [22]. Eriksen et al. further estimated PQ in cultivations of *Chlorella* sp. and *Chlamydomonas Reinhardtii* under different nitrogen sources and reported values of approximately 1.31, 1.14 and 0.95 for *Chlorella* sp. grown on NO_3^-, NO_2^- and NH_4^+ and a PQ ~1.05 for the growth of *Chlamydomonas Reinhardtii* using on NH_4^+ [27].

To better assess the different process stages, we determined the moving average of the continuously monitored PQ over 24-h time intervals. Although average PQs remained considerably constant over most of the process time at values around 1.25, this measure still allows for identifying different cell stages briefly. As can be seen in Fig. 5(A & B) PQ values quickly equilibrated in the exponential growth phase of the first two days. In the next process section, average PQ levels started to decline slightly but steadily until the 6th day of the experiments.

Next, the averaged PQ ratio rebounds and settles again at stable levels of around 1.18–1.27 for another 6 days before inclining significantly in the last process stage. These observations were made for all three cultivations comparably (Fig. 5B).

Another point of attention in this study was focused on a procedure for the on-line determination of nitrate uptake by the microalgae. Based on the stoichiometric proton imbalance effects, NO3 uptake was estimated utilizing on-line monitored data of acid addition, off-gas CO2 analysis, and pH measured in situ and employing Eqs. (16)–(19).

Results of the hourly and 24-h moving averages of estimated NO_3^--uptake rates are shown in Fig. 6. Noticeable at first sight are sharp peaks

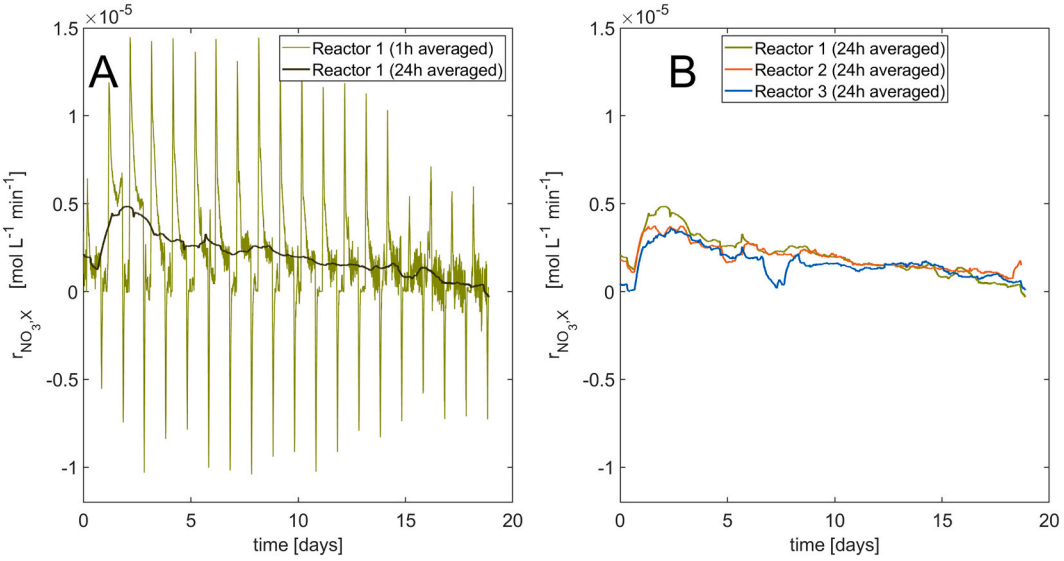


Fig. 6. Online estimated uptake rates of nitrate in microalgal batch cultivation (T. obliquus) based on mass and charge balance observations and nitric acid feed monitoring; (A): online estimated nitrate uptake rates in one cultivation as moving average over time intervals of 1 hour and 24 hours; (B): 24-hour moving averaged nitrate uptake rate estimated for three parallel cultivation for 16:8 hours Light: Dark (illumination block wise).

of NO_3 rates that appear within each day/night transition. Those peaks might be the result of inaccurately assessing the dynamics of mostly bicarbonate levels during these particular time intervals.

However, it appears that short overestimations of our nitrate rate estimates during the algal mornings are regularly followed up by similar underestimations in the transition to night. This suggests that estimation errors during one transition phase are being compensated over a 24 h period. However, trends in the hourly averaged uptake rates in Fig. 6A also indicate that nitrate uptake can be assumed to mostly occur during the day phase. Also, during the first three days of exponential growth nitrate uptake rates were observed to be considerably higher than in the later process stages which is reflected in both the hourly averaged and 24-h averages of nitrate uptake rates Fig. 6A & B. Between the first to the second day of cultivation when photon flux density had been increased by a factor of four nitrate uptakes were also seen to incline significantly. This reaction is later followed by a decrease in 24 h averaged assimilation rates. To the best of our knowledge no further studies have produced similar estimates of microalgal nitrate uptake at such high monitoring time resolution so far. Towards the end of the cultivation experiments signals of the nitrate uptake became increasingly more noisy. At this moment, nitrate consumption and growth had practically ceased so that the method probably approached its limit of detection.

3.3. Estimating biomass growth on-line

The most significant parameter in microalgal production is the assessment of growth, which is often presented in terms of biomass concentration.

The estimated biomass for the described process is displayed over process time in Fig. 7 for two reactors obtained via dry weight analysis of periodically taken samples and online monitoring using the previously described rate-based approach of estimation. All three on-line methods employed in this study were successful in depicting the dynamics of batch growth with its lag-phase, exponential phase, linear growth, and the transition into the stationary phase qualitatively (Fig. 7A, B & C). Estimates by on-line monitoring could be obtained in good agreement with the results obtained from dry weight analysis (Fig. 7D, E & F) respectively.

For the biomass determination via gas balancing of oxygen flows (Fig. 7A & B) deviating results of dry weights and online monitoring were obtained at approximately 6.7 % NRMSD for the two cultivations in sum. Moreover, the determined R^2 of 0.96 for this method showed a 'very good' correlation between the two methods. Interestingly, online estimation of the second cultivation process had predicted an exceedingly higher biomass concentration than was obtained by dry weight analysis towards the end of the process. A similar behavior was observed when biomass estimation was carried out on the basis of carbon dioxide balancing. In this approach, the biomass could be monitored with also 'very high' accuracy and precision, achieving overall values of ~0.94 R^2 and 7.1 % NRMSD. These were comparable performance values to those obtained from the oxygen signal.

In comparison, predictions of accrued biomass on the basis of charge balancing (Fig. 7E & F) generally yielded slightly higher estimates of biomass than were achieved by the gas balancing methods (Fig. 7A & C). With respect to DW, we determined ~7.5 % of deviation (NRMSD). Nevertheless, the R^2 of 0.96 still showed a very good correlation (Fig. 7F) of this online monitoring tool. In contrast to the other two methods, this method did not determine the biomass growth of the second reactor to surpass the concentrations of the first one.

In order to elaborate on the performance of the different monitoring approaches tested, several aspects should be taken into account first to fairly expand on strengths and weaknesses between different monitoring

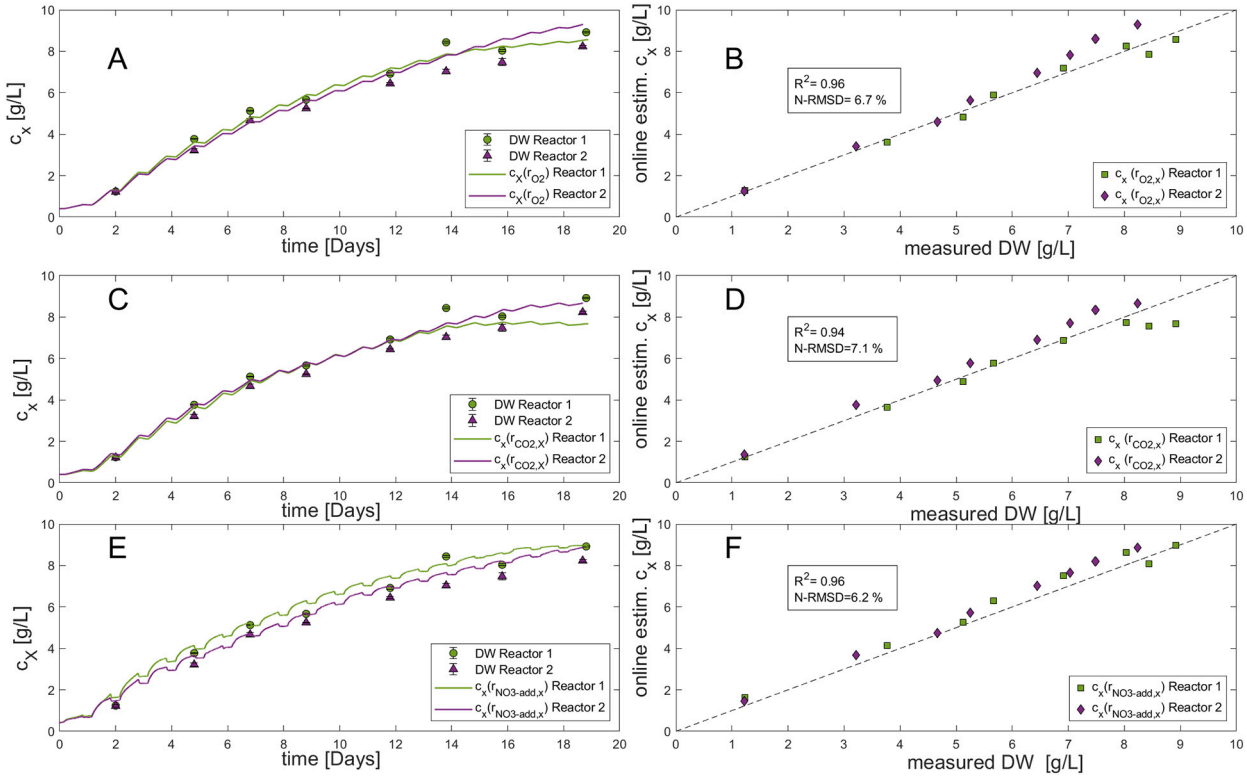


Fig. 7. Development of biomass growth over time in duplicate Batch cultures of Tetradesmus obliquus determined by three different online monitoring methods and correlation graphs of on-line obtained results with off-line measurements of Dry weight (DW). (A): Biomass determined by oxygen balancing and DW measurements; (B): correlation between oxygen production based c_X estimations and DW; (C): Biomass determined by carbon balancing and DW measurements; (D): correlation between CO_2 uptake based c_X estimations and DW; (E): biomass determined by nitrate balancing and DW measurements; (F): correlation between nitrate uptake based c_X estimations and DW.

strategies.

First, different monitoring techniques rely on varying assumptions of idealistic process scenarios. Although measuring cell dry weights over process time is commonly used to represent the dynamics of growth processes and determine key process variables, it is based on an assumption of perfect, homogeneous mixing in the reaction volume. This assumption is often oversimplifying given that many microalgae tend to flocculate, adhere on surfaces, or sediment to the ground. Moreover, most reaction systems for microalgal cultivation make use of rather gentle kinetic energy input and are designed to maximize surfaces to assure high light transport into the culture. This makes it very difficult to verify homogenous mixing. Probably, in many cases, growth in biofilms and sedimentation processes cannot be determined accurately. Estimates of the produced biomass obtained from sampling and subsequent analysis of CDW or optical density (OD) would, in consequence, understate the actual productivities achieved in the reactor.

During the three cultivation processes, we observed similar effects despite the use of a magnetic window cleaner that had been placed in the reactor to remove biofilms and homogenize cultures before withdrawing samples. It can therefore be assumed that the cell dry weight estimates, especially in the later process stages, tend to underestimate the net growth. However, CDW and OD measurements are widely applied in research and industries because they are low-cost, easy to conduct, and considerably reproducible.

Regarding the online monitoring strategies via mass and charge balancing introduced in this study, we would like to emphasize some factors we understand as prerequisites denominating the success of elemental-mass-balancing for growth tracking. During the biomass determination via gas flow analysis, several assumptions were made. These include assumptions of instantaneous and perfect mixing of inlet gas streams in the gas phase. That means that saturation dynamics in the gas volume and the increased gas retention time were not taken into account. Although being negligibly small at the laboratory scale of 1.8 L volume, these effects could become more important in larger systems. Moreover, we assumed that both oxygen and carbon dioxide behave like ideal gases which is another simplification considered.

In this study, three different reactors were used, each one equipped with its own set of mass flow controllers. These controllers are calibrated annually at our laboratories. However, even small but systematic errors in the assumed flow rates of gases would propagate due to the time-wise integration of conversion rates for biomass prediction. If not handled properly, this can result in increasing inaccuracy of biomass estimates using the rate-based on-line monitoring at longer process time. Nonetheless, an advantage of non-invasive use of gas analysis is that recalibration and verification of actual gas flows can be carried out mid-experiment without significant interference.

Another possible source of error lies in the choice of the stoichiometric model, which builds the foundation to derive variables of formed biomass from volumetric conversion rates.

In this study, we utilized a model composition developed by Kliphuis et al. for cultures of *Chlorella sorokiniana* grown under continuous illumination [22]. Elemental composition analysis of microalgae has already been the object of intensive investigation among researchers ([27–30]). Therefore, multiple composition models have been proposed either for specific strains or as generic representations of microalgal biomasses as listed in Table 1. Unfortunately, cultivation strategies, techniques of element analysis, and the respective results differ considerably. A standardized methodology and interpretation of data often still has to be agreed upon. Even more, it should be considered that the constants of the microalgal composition may not at all be a reasonable concept in the first place. On the contrary, it might rather be a broad oversimplification of way more complexly distributed natural phenomena in the growth process of cells.

Table 1
Reported stoichiometric composition and model composition for different freshwater microalgae and generic representation microalgae normalized to total Carbon content (1 Cmol-X).

Microalgae	Composition	Reference
S. obliquus	$CH_{1.64}O_{0.49}N_{0.10}$	[28]
S. obliquus (CNW-N)	$CH_{1.86}O_{0.51}N_{0.16}$	[29]
Chlorella sorokiniana	$CH_{1.7}O_{0.4}N_{0.15}$	[22]
Chlamydomonas Reinhardtii	(Range) $CH_{1.71–1.96}O_{0.53–0.82}N_{0.02–0.13}$	[27]
Generic	$CH_{1.63}O_{0.4}N_{0.185}P_{0.045}$	[30]

In that light, we reckon the elemental composition, as proposed by Kliphuis et al., a reasonable compromise and probably suitable for representing average freshwater microalgae [22]. This is also supported by the accuracy obtained from the online monitoring tools described in this study.

However, strain-specific differences in the biomass composition, specifically C: N and C:O ratios, could have affected the outcome of monitoring. In addition, differences in cultivation conditions, such as continuous versus periodic illumination, could have also impacted microalgal stoichiometry.

This theory is, at least, supported by the fluctuations that were found in hourly and 24-h averaged PQ values, shown in Fig. 5. According to our stoichiometric assumption (Eq. (3)), we expected approximately 1.4 mol of oxygen to be released per mol of captured CO_2. Plateaus of PQ during day phases reached comparable values close to this hypothesized ratio. Nevertheless, daily averaged PQ values, on the other hand, were found to be significantly lower at around PQ of 1.16–1.27, which is up to 18 % lower than assumed by the model equation. The stoichiometric model might, therefore, be better suited to represent photosynthesis phases solely. In retrospect, this means that for improving monitoring accuracy, the constantly assumed biomass model composition should reflect conditions of fluctuating day-night regimes.

The validation of sensing performance, monitoring accuracy, and reliability in this study was conducted with respect to cell dry weight measurements. This metric is usually considered the 'golden standard' in bioprocess technologies.

Another option for tracking biomass growth involves measuring light absorbance and optical density (OD) of cell cultures. This tool is often faster in determining estimates of biomass concentrations. Some common drawbacks of OD measurements are the required withdrawal of the sample, necessary dilution, and the need to build a correlating function to biomass concentrations empirically. The last aspect usually requires additional calibration efforts before the cultivation. Mid-process affected changes in some biomass properties, such as the cell morphology, aggregation, and pigment contents [31], can render those calibrations outdated and unfeasible to reliably estimate biomass [6].

The manual sampling further increases the risk of process contamination. Displayed in Fig. 8 are correlations that were drawn between estimated biomass levels by means of online mass balancing and OD750 measurements as opposed to Dry weights. As can be seen, biomass concentrations can be determined very accurately by measuring OD_{750} provided that the conversion factor of absorbance and CDW is known.

Calibrations require effort and time to produce multiple points of measurement and perform the linear regression. Nevertheless, this procedure also enables corrections for systematic disturbances that might have been overlooked.

A direct comparison between OD_{750} estimates and the rate-based online monitoring methods would, therefore, be inadequate since the online approaches do not rely on a direct validation procedure. Consequently, we employed a fitting by linear regression to the online estimates of biomass to be able to elaborate on the true potential of these tools. Depicted in Table 2 are the obtained values for R^2 and N-RMSD of online estimated algal concentration by the unfitted correlation and corrected via linear regression for each reactor and method separately.

Noticeably, R^2 coefficients of determination could be improved by the linear regression fits in all on-line mass-balancing methods employed. This indicates that on-line monitoring via mass and charge

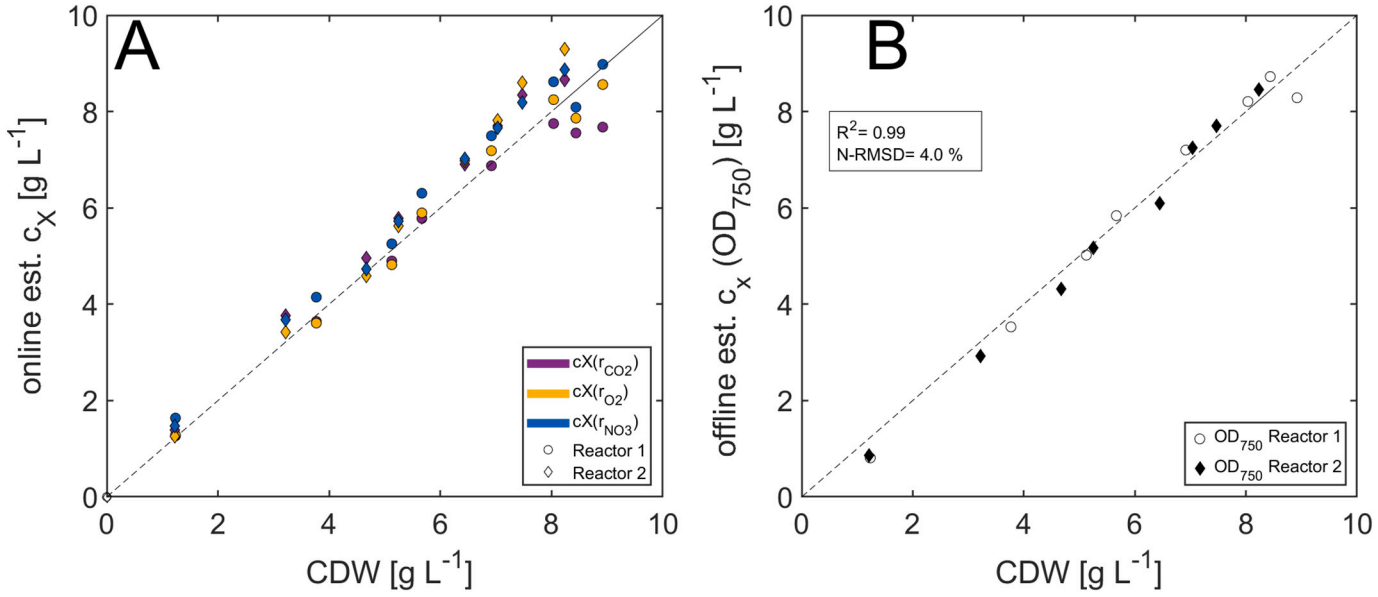


Fig. 8. correlation of results using different estimation strategies to determine biomass concentrations in two batch cultivation of Tetradesmus obliquus; (A): online estimates of C_X by different online mass balance approaches of monitoring vs Cell dry weight (CDW) results; (B): correlation of biomass estimates using optical density measurements at 750 nm wavelength (OD750) converted to weight estimates by linear regression fit to CDW.

Table 2
Estimation accuracy indicators (R^2 and N-RMSD) normalized Root mean square deviations with respect to measured Cell Dry Weights (CDW) for biomass concentration estimates by on-line monitoring rates of volumetric carbon dioxide, oxygen and nitric acid transfers and mass-charge-balancing.

Estimation method for C_X		R^2 (unfitted estimates)	N-RMSD [%] (unfitted estimates)	R^2 of fit	N-RMSD of fit [%]
CUR	Reactor 1	0.95	7.6	0.995	5
	Reactor 2	0.936	7.3	0.972	2.6
OPR	Reactor 1	0.938	9.3	0.99	4
	Reactor 2	0.98	3.98	0.986	4
Nitrate uptake rate	Reactor 1	0.907	10.5	0.988	6.3
	Reactor 2	0.933	7.91	0.961	3.9
OD750	Reactor 1	–	–	0.989	4.3
	Reactor 2	–	–	0.990	3.9

balances can be employed to monitor microalgal growth at a similar accuracy and reliability as the established techniques of cell dry weight or optical density measurements.

As we intended to propose novel on-line monitoring tools that allow for the continuous and reliable assessment of microalgal growth, we considered the factor of measurement repeatability as equally important as accuracy. Outlining the ability to reproduce measurement results is important to establish trust in the experimentally obtained data. In that context, rate-based online monitoring tools hold a major disadvantage in that the monitoring is usually not performed in triplicate. Measurement 'outliers', signal abnormalities, or other unexpected behavior can thus often not be reasonably excluded by statistical means, nor can they be trusted with confidence, since the failure of sensors is always a possible explanation. In the case of the rate-based parameter estimation, such events would be even more intricate due to the 'memory' function of the integration terms. For this reason, 'measurement redundancy', as a strategy of performing multiple parallel determinations of single process variables, is the suggested instrument of choice. By measurement redundancy in monitoring systems faulty readings can be detected and excluded.

To implement measurement redundancy properly it should be aimed for combination of different principles employed in order to minimize the probability of biases. In this study we already proposed three considerably different approaches for biomass estimations. Thereby we had implemented measurement redundancy to assess the growth of *T. obliquus* in batch cultures reliably. For this reason, we determined in a third cultivation to track only the batch growth by means of the three online mass balancing tools of biomass monitoring. This was supported by determining the biomass concentration via DW analysis exclusively at the end of the Cultivation. Developments of the tracked biomass growth monitored by the trinity of on-line measurements are shown in Fig. 9. Despite the failure of a light control system, and the consecutive elongation of one night phase between day 6 and 8 estimations by all three online methods was obtained in reasonable agreement. A precise quantification of the microalgal biomass concentrations could be made at any given time point of the 18-day-long process instantaneously and with confidence by the triplicate of measurements. The process monitoring was conducted fully automated and with no manual interference to the process.

Although the presented outcomes on precision and accuracy of the presented rate-based online monitoring approaches seem very promising, several aspects of this technology have to be critically reflected on. A key aspect for evaluation might be the broadness of applicability in different areas of microalgal process industries. So far, the monitoring approach has only been validated in a semi-closed system in which gas transport could be assessed directly. All experiments were exclusively performed in bench-scale reactors of 1.8 L volume, where mixing was assumed to be instantaneous and homogenous. Lastly, the approach had been tested for an axenic cultivation of *T. obliquus*, representing a model organism for freshwater conditions. In contrast, industrially relevant microalgal applications are often carried out under nearly opposite set of conditions. The industrial scale of microalgae cultivation often reaches magnitudes of several thousand liters in reactor volume. Furthermore, processes such as the microalgal wastewater treatment are run in open systems where gas loss to the atmosphere is difficult to determine accurately, and axenic cultivation is nearly impossible. Overcoming

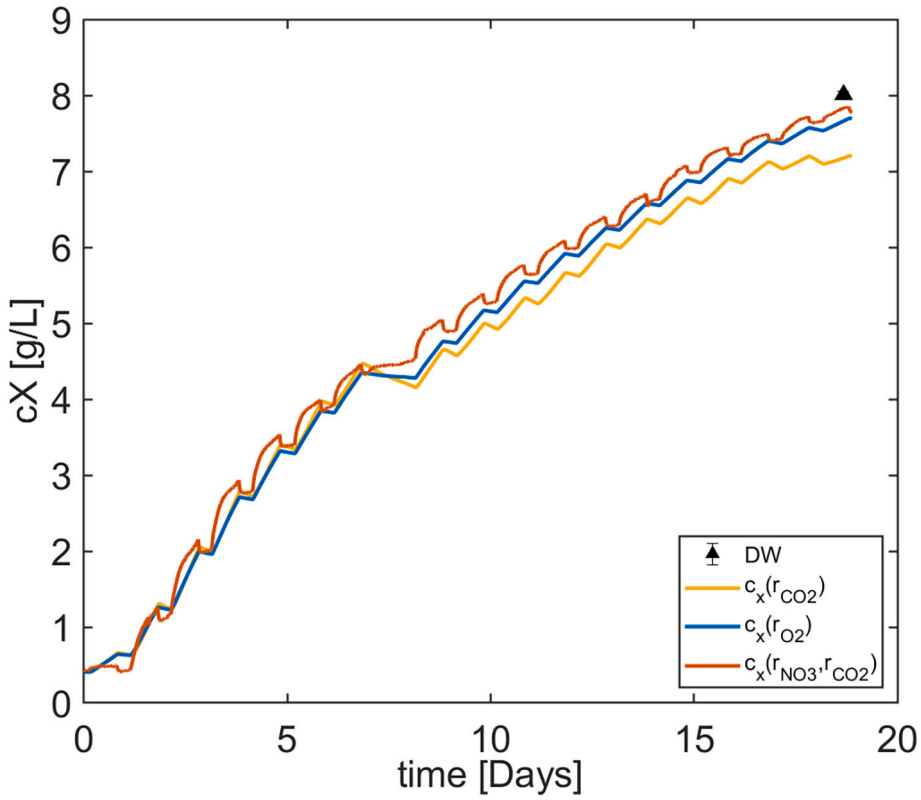


Fig. 9. Biomass growth of a cultivation of Tetradesmus obliquus in a 1.8 L flatpanel photobioreactor in batch-model assessed by three different methods of online monitoring based on mass and charge balancing principles; Respective signal input for the estimates were data of either: $c_{CO2,gas}$; $c_{O2,Gas}$ or a combination of the measured CO2-Gas fraction, pH and HNO_3-solution supply.

these hurdles requires additional detailed knowledge and characteristic models on mixing behavior, residence time distribution, and signal propagation delay between actuator controls and measurements. Even further, variations in temperature due to weather influences can impact the saturation concentration and thereby the dynamics of gas transport to and from the medium, which needs to be accounted for. Applying this monitoring approach in open cultivation systems would also require changes to the measurement devices employed. For instance, switching from off-gas analyzers to submerged sensors of dissolved oxygen and CO_2 would be needed.

Probably the most intricate aspect, however, is posed by the mix-culture behavior of e.g. wastewater treatments, where measured nutrient conversion rates can not exclusively be associated with the growth of microalgae. The stoichiometric description of the process might, in that case, involve multiple equations to model the different key biological reactions in the mixture. Nevertheless, the proposed monitoring strategy might be extendable to open systems as it determines multiple rates, thus allowing to solve equation systems with multiple outputs. In that light, it should be emphasized that other measurement techniques struggle with similar issues in such complex reaction systems.

4. Conclusions

This study presents three distinctive strategies for non-invasive online monitoring of microalgal growth processes based on mass and charge balances utilizing measurements of CO_2 and O_2 gas analysis, nitric acid supply, and pH as input. All three monitoring tools proved suitable for the automated monitoring of microalgal biomass growth, with a very good correlation to dry weight measurements of biomass performed offline over several weeks of cultivation. Each method proposed consists of two steps. The first step estimates the growth-associated conversion rate of a key molecular component, and the second step determines the corresponding formation of biomass based on a stoichiometric model of microalgal biomass composition. Aside from accurate biomass monitoring, this strategy also enables the identification of different cell and process states of microalgae in batch cultivations with light as the limiting parameter. The proposed on-line monitoring methods can be integrated and combined simultaneously in closed photobioreactor systems for improved reliability and cell state monitoring. These approaches thereby provide valuable groundwork for automating monitoring and control systems of microalgal processes.

CRediT authorship contribution statement

Henrik Geltner: Writing – original draft, Visualization, Software, Methodology, Investigation, Formal analysis, Data curation, Conceptualization. **Sjoerd Kortstee:** Methodology, Investigation. **Maria Barbosa:** Writing – review & editing, Supervision, Funding acquisition. **Marcel Janssen:** Writing – review & editing, Supervision, Conceptualization.

Declaration of Generative AI and AI-assisted technologies in the writing process

Statement: During the preparation of this work the author(s) used Grammarly in order to improve the readability. After using this tool, the author(s) reviewed and edited the content as needed and take full responsibility for the content of the published article.

Funding

This work was supported by the European Union's Horizon 2020 research and innovation program under the Marie Skłodowska-Curie

grant agreement N° 955520 (DigitAlgaesation).

Declaration of competing interest

The authors declare that they have no known competing financial interests or personal relationships that could have appeared to influence the work reported in this article.

Data availability

Data will be made available on request.

References

[1] J. Ullmann, D. Grimm, Algae and their potential for a future bioeconomy, landless food production, and the socio-economic impact of an algae industry, Bd 11 (2021) 261–267.

[2] I. Havlik, T. Scheper, K.F. Reardon, Monitoring of microalgal processes, in: Microalgae Biotechnology, Springer International Publishing, 2015, pp. 89–142.

[3] M. Janssen, R.H. Wijffels, M.J. Barbosa, Microalgae based production of single-cell protein, Bd 75 (2022) 102705.

[4] I. Havlik, P. Lindner, T. Scheper, K.F. Reardon, On-line monitoring of large cultivations of microalgae and cyanobacteria, Bd 31 (2013) 406–414.

[5] M. de Sa, Monitoring of Biological Processes in Microalgae Production Using Fluorescence Spectroscopy, Facultad De Ciencias E Tecnologia, 2019.

[6] I. Havlik, S. Beutel, T. Scheper, K.F. Reardon, On-line monitoring of biological parameters in microalgal bioprocesses using optical methods, Energies 15 (January 2022) 875. Bd.

[7] C. Lieutaud, A. Assaf, O. Gonçalves, G. Wielgosz-Collin, G. Thouand, Fast non-invasive monitoring of microalgal physiological stage in photobioreactors through Raman spectroscopy, Algal Res. 42 (September 2019) 101595. Bd.

[8] D. Morgado, A. Fanesi, T. Martin, S. Tebbani, O. Bernard, F. Lopes, Non-destructive monitoring of microalgae biofilms, Bioresour. Technol. 398 (April 2024) 130520.

[9] M. Dabros, M. Amrhein, D. Bonvin, I.W. Marison, U. von Stockar, Data reconciliation of concentration estimates from mid-infrared and dielectric spectral measurements for improved on-line monitoring of bioprocesses 25 (March 2009) 578–588.

[10] V. Brunner, L. Klöckner, R. Kerpes, D.U. Geier, T. Becker, Online sensor validation in sensor networks for bioprocess monitoring using swarm intelligence 412 (2020) 2165–2175.

[11] R. Bleisch, G. Mühlstädt, G. Hilpmann, L. Seibel, J. Steingröwer, S. Zahn, A. M. Wagemans, F. Krujatz, A robust, non-invasive and fast routine for the quantification of the nutritional composition of microalgae biomass slurries based on near-infrared spectroscopy, Algal Research 85 (January 2025) 103882.

[12] C. Herwig, I. Marison, U. von Stockar, On-line stoichiometry and identification of metabolic state under dynamic process conditions 75 (2001) 345–354.

[13] F. García-Mañas, J.L. Guzmán, M. Berenguel, F.G. Acién, Biomass estimation of an industrial raceway photobioreactor using an extended Kalman filter and a dynamic model for microalgae production, Algal Research 37 (January 2019) 103–114.

[14] M. Sá, N. Ferrer-Ledo, F. Gao, C.G. Bertinetto, J. Jansen, J.G. Crespo, R.H. Wijffels, M. Barbosa, C.F. Galinha, Perspectives of fluorescence spectroscopy for online monitoring in microalgae industry, J. Microbial. Biotechnol. 15 (February 2022) 1824–1838.

[15] M.L. Scherholz, W.R. Curtis, Achieving pH control in microalgal cultures through fed-batch addition of stoichiometrically-balanced growth media, BMC Biotechnol. 13 (May 2013).

[16] J. Wang, W.R. Curtis, Proton stoichiometric imbalance during algae photosynthetic growth on various nitrogen sources: toward metabolic pH control, Journal of Applied Phycology 28 (April 2015) 43–52.

[17] F. Mairet, M. Moisan, O. Bernard, Estimation of neutral lipid and carbohydrate quotas in microalgae using adaptive interval observers, Bioprocess Biosyst. Eng. 37 (February 2013) 51–61.

[18] G. Breuer, P.P. Lamers, D.E. Martens, R.B. Draaisma, R.H. Wijffels, The impact of nitrogen starvation on the dynamics of triacylglycerol accumulation in nine microalgae strains, Bioresour. Technol. 124 (November 2012) 217–226.

[19] M. Cuaresma, M. Janssen, C. Vílchez, R.H. Wijffels, Horizontal or vertical photobioreactors? How to improve microalgae photosynthetic efficiency 102 (2011) 5129–5137.

[20] W. M. Haynes und D. R. Lide, Hrsg., CRC Handbook of Chemistry and Physics, 93. ed., 2012 - 2013 Hrsg., Boca Raton, Fla. [u.a.]: CRC Press, 2012.

[21] J. Vanags, A. Suleiko, Oxygen mass transfer coefficient application in characterisation of bioreactors and fermentation processes, Latv. J. Phys. Tech. Sci. 59 (October 2022) 21–32.

[22] A.M.J. Kliphuis, L. de Winter, C. Vejrazka, D.E. Martens, M. Janssen, R.H. Wijffels, Photosynthetic efficiency of Chlorella sorokiniana in a turbulently mixed short light-path photobioreactor, Biotechnol. Prog. 26 (February 2010) 687–696.

[23] A.M.J. Kliphuis, M. Janssen, E.J. van den End, D.E. Martens, R.H. Wijffels, Light respiration in Chlorella sorokiniana, Journal of Applied Phycology 23 (November 2010) 935–947.

[24] M. Janssen, Microalgal Photosynthesis and Growth in Mass Culture (2016) 185–256.

[25] Bo-Ping Han, A mechanistic model of algal Photoinhibition induced by Photodamage to photosystem-II, J. Theor. Biol. 214 (February 2002) 519–527.

[26] P.J. Nixon, F. Michoux, J. Yu, M. Boehm, J. Komenda, Recent advances in understanding the assembly and repair of photosystem II, Ann. Bot. 106 (March 2010) 1–16.

[27] N.T. Eriksen, F.K. Riisgård, W.S. Gunther, J.J. Lønsmann Iversen, On-line estimation of O2 production, CO2 uptake, and growth kinetics of microalgal cultures in a gas-tight photobioreactor, J. Appl. Phycol. 19 (November 2006) 161–174.

[28] J.L. Zelibor, L. Romankiw, P.G. Hatcher, R.R. Colwell, Comparative analysis of the chemical composition of mixed and pure cultures of green algae and their decomposed residues by ¹³C nuclear magnetic resonance spectroscopy, Appl. Environ. Microbiol. 54 (1988) 1051–1060.

[29] W.-H. Chen, Z.-Y. Wu, J.-S. Chang, Isothermal and non-isothermal torrefaction characteristics and kinetics of microalga Scenedesmus obliquus CNW-N, Bioresour. Technol. 155 (March 2014) 245–251.

[30] M.T. Myint, A. Ghassemi, N. Nirmalakhandan, A generic stoichiometric equation for microalgae–microorganism nexus by using clarified domestic wastewater as growth medium, Desalin. Water Treat. 51 (October 2013) 6632–6640.

[31] M.J. Griffiths, C. Garcin, R.P. van Hille, S.T.L. Harrison, Interference by pigment in the estimation of microalgal biomass concentration by optical density, J. Microbiol. Methods 85 (May 2011) 119–123.